Clinics of Oncology

Research Article ISSN: 2640-1037 |Volume 8

Low Cohesive Gastric Cancer of the Antrum and Duodenum. Multi-omics analysis Can it Improve Treatment?

Joaquín Losada[1*], Aingeru Sarriugarte[2], Esther Irizar[3], Begoña Maestro[4], Isami Soeda[5] and Ines Losada[6]

[1]Department of Neuroscience UPV/EHU, Zorrotzaurre Clinic, Spain

[2]Department of Surgery, Cruces University Hospital, Zorrotzaurre Clinic, Spain

[3]Department of Pathology, Zorrotzaurre Clinic, Spain

[4]Department of Anaesthesia, Basurto Universitary Hospital, Zorrotzaurre Clinic, Spain

[5]Department of Surgery, Txagorritxu Universitary Hospital, Spain

[6]Department of Internal Medicine, Son Llátzer University Hospital, Balearic Island University, Spain

[*]Corresponding author:

Joaquín Losada,
Department of Neuroscience UPV/EHU,
Zorrotzaurre Clinic, Spain

Received: 26 Dec 2024
Accepted: 06 Jan 2025
Published: 11 Jan 2025
J Short Name: COO

Keywords:

Low cohesive gastric carcinoma; Epigenetic biomarkers; Multi-omics analysis; Precision treatment

Citation:

Joaquín Losada, Low Cohesive Gastric Cancer of the Antrum and Duodenum. Multi-omics analysis Can it Improve Treatment?. Clin Onco. 2025; 8(5): 125

1. Abstract

Four patients with poorly cohesive gastric cancer were studied. The types analyzed included the intestinal (C1), signet ring cells (C2 and C4), and unspecified (C3). Patient C4 showed duodenal infiltration from the gastric antrum. Despite several diagnostic tests and treatments, it was not possible to determine the extension of the tumor to the duodenum or to improve the patient's prognosis. Sequencing of the tumor identified mutations in CREBBP, whose variant presented a substitution of arginine for cysteine, and the mutation in the TP53 oncogene did not change the position of the amino acid threonine (Thr125=). C1, C2 and C3 cases were subjected to proteomic analysis in healthy and tumor gastric tissues. Proteins associated with the CREBBP and TP53 genes, other proteins associated with arginine and cysteine, histones HAT and HDAC, and proteins of the ubiquitin-proteasome system were examined. Using the XLSTAT program, significant differences in the expression of SDCBP, NCBP1, MGMT, RARS, HDAC1, UBE1 and UBE2K proteins were observed, highlighting their potential as biomarkers for this type of gastric cancer. In experimental studies, Inobrodib showed efficacy in modulating P300/CBP and the use of mc-tRNA to correct amino acid errors caused by mutations. In addition, it has been suggested that targeted protein degradation (PROTAC) focusing on key proteins and epigenetic factors may offer new therapeutic alternatives. Therefore, it is recommended to review and adapt diagnostic and therapeutic strategies for the diagnosis and treatment of poorly cohesive gastric cancer based on these findings.

2. Introduction

Diffuse gastric cancer in Lauren's classification corresponds to with low cohesive gastric carcinoma (GC-PCC) in the World Health Organization (WHO) classification [1]. It tends to develop in women before the age of 40 years while, above this age, it is more frequent in men [2]. In recent decades the overall incidence of gastric cancer (GC) has decreased worldwide, however, signet ring cell GC-PCC has increased [3]. The Verona consensus proposed reclassifying CG-PCC, with more than 90% signet ring cells (SRC) as signet ring cell CG-PCC. The other two categories were poorly cohesive with less than 90% SRC component, but more than 10% and poorly cohesive not specified (PCC-NOS), with less than 10% SRC [4]. Analysis of the TCGA Pan-Cancer Atlas, which is available on cBioPortal for Cancer Genomics and specifically focused on gastric cancer (OncoSG, 2018), has determined that CREBBP gene mutations occur at a frequency of 4.10%. In contrast, TP53 gene mutations occur with a frequency of 47%, within the set of mu-

tated genes analyzed in gastric cancer [5]. Histone modifications include processes such as methylation, acetylation and ubiquitination. Acetylation is an expanding repertoire of histone acylation that regulate chromatin and transcription [6]. The nuclear protein Q927393 CBP Human is a CREBBP gene-binding protein (NCBI 1387) that acts as a histone acetyl transferase transcriptional coactivator [7]. P300 (KAT2B) is closely related to CREBBP-binding protein, also known as (KAT2A) [8]. CREBBP and P300 gene, produce increased histone acetylation, which promote cancer metastasis, immune evasion and drug resistance [9]. The E1A acetyltransferase-binding protein P300 (EP300 or KAT2B) is one of the HATs altered in intestinal and diffuse gastric cancer [10]. Various genetic mutations and epigenetic modifications can alter the function of histone acetyltransferases (HATs) [11]. Examples of epigenetic regulators are histone acetylates, such as CREBBP and histone deacetylases, such as HDAC1. These regulate one or more types of modifications, most of which are involved in the genesis or progression of GC [12]. In addition, the p53 gene (NCBI 7157) is a type of tumor suppressor gene, also called p53 tumor protein gene, which encodes a nuclear transcription factor. Both genes are involved in GC genesis. Another factor in tumor development is metabolic reprogramming. Altered L-arginine metabolic pathways are potential therapeutic targets and biomarkers in gastric cancer [13]. Increased plasma arginine level in gastric cancer patients was associated with overexpression of arginine succinate synthase 1 (ASS1). Elevated ASS1 expression is associated with increased survival in patients with gastric cancer. In addition, pretreatment arginine levels could serve as prognostic factor [14]. The clinical practice guideline for the diagnosis and treatment of gastric cancer, developed by the European Society for Medical Oncology (ESMO) and Pan-Asian (PAGA) for the diagnosis of metastatic or inoperable gastric cancer, it is recommended to determine the molecular profile of each individual tumor. This includes expression by immunohistochemistry and/or in situ hybridization amplification of ErbB-2 (P04626) receptor tyrosine kinase (ERBB2) protein (Her2 gene), programmed cell death ligand 1 (PD-L1) and microsatellite high instability/high deficiency (MSI-H) status. It also recommends examining the expression of Claudin-18 by immunohistochemistry [15]. The molecular data provided by the guidelines do not seem sufficient to cover the diagnostic and treatment needs of all GC subtypes. Given the potential of multi-omics technology, its incorporation would be useful to improve the diagnosis and treatment of these patients. Although the economic and validation challenges involved are recognized, the progressive integration of these advances could offer significant benefits in the treatment of the disease. Next-generation sequencing and mass spectrometry have expanded GC capabilities to study the genome, epi-genome, transcriptome, miRNAs, immunity, microbiome, proteome and metabolome. Some of the epigenetic regulators involved in GC biology are DNA methylation, histone acetylation or ubiquitination, which can alter the DNA accessibility of transcription factors [16]. Most human genes with multiple exons have different isoforms, often resulting in different versions of the same protein [17]. The Cancer Genome Atlas (TCGA) revealed that functional effects of isoform changes by ubiquitination (E1, E3, E2, E4) and deubiquitinating (DUB) mechanisms influence the stability of quantification values of oncogenic and tumor suppressor proteins such as those in diffuse gastric cancer [18]. The CREBBP gene, although is not a direct part of the Ubiquitin-Proteasome System (UPS), influences its activity for being a target of UPS degradation and maintaining the balance in the expression of pro- and anti-apoptotic proteins, which interact with the UPS. The ubiquitination pathway plays a role in the development of GC, so that therapies that modulate UPS could be effective in the treatment. However, this strategy is feasible only, if the mutation of the gene in the GC-PCC tumor cell results in an increase of function. If histopathological classifications with molecular classifications are compared in CG, although they are complementary, molecular classifications have a greater clinical impact. Since they enable a more accurate diagnosis, patients' treatment and prognosis [19] could be predicted. The translation of basic research into clinical practice offers a real opportunity for patients. The hypothesis suggests that the incorporation of multiomic analysis by multidisciplinary medical teams treating these patients could significantly improve clinical outcomes.

3. Objective and Approach

a) Analyze the quantification values of CBP proteins and those involved in the metabolism of the amino acids Arginine and Cysteine, in the different subtypes of CG-PCC. b). Analyze the quantification values of the TU/SA (Tumor/Sane) ratio of proteins involved in histone acetylation and proteins of the ubiquitination system (USB) and that influence or not in the pathogenesis of the different subtypes of GC-PCC. c) Improve the diagnostic and therapeutic efficacy of GC-PCC with the bio-statistical analysis of the quantified proteins.

4. Cases Reports

4.1. Oncological History and Case 4

A 44-year-old woman with no past medical history presented with localized pain in the epigastric region. The physical examination was normal. Gastroscopy revealed an extensive tumor in the gastric antrum affecting the entire gastric wall and extended into the duodenum. A biopsy was performed.

4.2. Biopsy Results

Microscopic anatomy, hematoxylin, and eosin staining showed a gastric antrum mucosa with chronic and acute inflammation (Figure 1a). There was an extensive infiltration of the own lamination by a carcinoma composed predominantly of signet ring cells with cytoplasmic mucin and a displaced nucleus (Figure 1b). It showed a diffuse infiltrative pattern of cell cord distribution (Figure 1c)), with two foci of cells with marked anaplasia (Figure 3d)). The his-

topathologic diagnosis was GC-PCC with a predominance of signet ring cells. Immunohistochemistry identified Helicobacter pylori-like bacillus in more than 2/3 of the gastric mucosa of CG-PCC case 4, (Figure 1 e), (Appendix 1). HER2 expression in the gastric tumor was positive, with an extensive cluster of cancer cells with strong immuno-reactivity at the cell membrane. The antibody used for immunostaining was Ab268053 anti-ErbB2 / HER2 antibody [ERBB2/3093]. In addition, histological tumor sections placed on slides expressed PD-L1 measured by the combined positive score (CPS). It had a positive expression level equal to or greater than one (5.0). An anti-PD-L1 monoclonal antibody, specifically IHC 28-8 pharm DxSK005, was used, which was applied by means of an Autostainer Link 48.

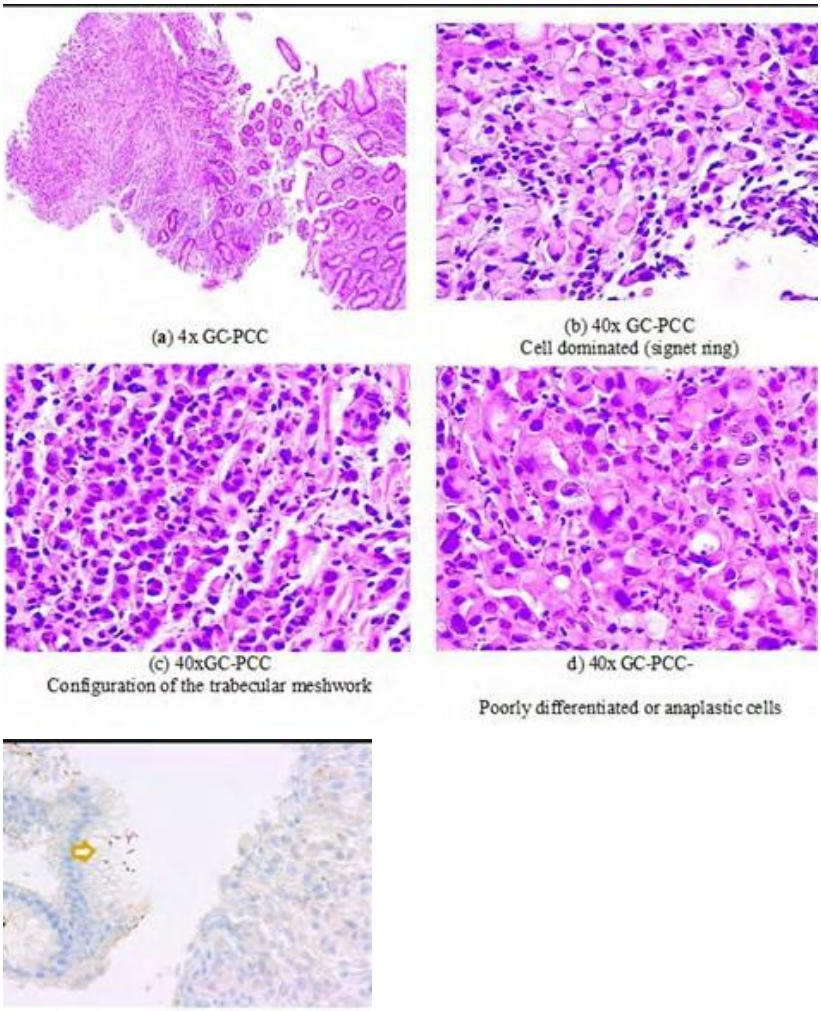

Figure 1E

4.3. Surgery and Chemotherapy

The patient referred to the oncologic medical history. In February 2024, an exploratory laparoscopy was performed, where no free peritoneal fluid was observed or macroscopic lesions in the peritoneum or in the round ligament were found. Brushing of the anterior aspect of the gastric antrum and round ligament showed negative cytology for malignant tumor cells. In March 2024, he started neo-adjuvant chemotherapy treatment in two cycles with Fluorouracil, Leucovorin, Oxaliplatin and Docetaxel, administered every two weeks. At the end of the second cycle of treatment, the patient went to the Medical Oncology office in April 2024, reporting abdominal distension and vomiting. Therefore, an abdominal-pelvic CT scan which showed a neoplastic stenosis at the level of the gastric antrum and pylorus with marked gastric dilatation without evidence of tumor dissemination was performed, (Figure 2a and 2b), (Appendix 1). The clinical evolution of the obstructive gastroduodenal process was not satisfactory, so in April 2024 she underwent exploratory laparotomy, which revealed an anthropiloric tumor with extension to the bulb and first duodenal knee, as well as infiltration of the head of the pancreas and structures of the hepatic hilum. Given that a R0 resection was not feasible, a retro gastric, ante colic, lateral gastroyeyunostomy was performed. In late April 2024, she was hospitalized again, for intestinal obstruction and underwent a laparotomy. During the operation, it was identified an internal hernia of Petersen's space with strangulation of a segment of small intestine through the defect between the alimentary loop

mesentery and the transverse meso-colon. The operation consisted of the hernia correction and closure of the Petersen's defect. Samples of the omental tissue were taken for histopathological analysis, which were negative. The postoperative progress was satisfactory. In May 2024, he started postoperative chemotherapy with Folfox and Trastuzumab until the beginning of July 2024. After completion of chemotherapy, a PET-CT scan was performed, the results of which are shown in (Figure 3 (a) and (b), (Appendix1). She was surgically re-intervened with R0 intention at the end of August 2024. The operative findings showed a gastric antrum tumor, surpassing the pylorus, with lateral extension to the upper knee of the duodenum. Implants in the peri-gastric peritoneal serosa were found and in the meso of the previous gastrojejunostomy loop. In addition, there was infiltration of the mesenteric wall of the transverse colon and its meso, which was adhered to the head of the pancreas. During surgery, doubts arose about the feasibility of the resection, due to a possible infiltration of the distal border of the duodenum and the possibility of requiring a cephalic duodeno-pancreatectomy. Also, because of the complications risk, even without achieving an R0 resection. The surgical intervention consisted of a 2/3 subtotal gastrectomy with distal duodenal section, D2 lymphadenectomy, cholecystectomy, resection of a fragment of the colon wall and transverse meso-colon and epiploectomy. Reconstruction by Roux-and-Y gastrojejunostomy was performed, duodenal closure with Echelon, and raffia of the transverse colon. The perioperative pathological anatomy revealed the lateral extension of the tumor into the duodenum, with infiltrated resection border. Given the existence of local peritoneal disease, a duodeno-pancreatectomy was discarded.

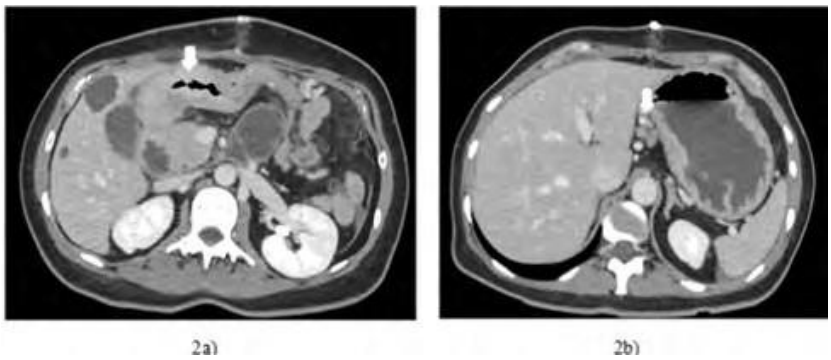

Figure 2a and 2b.

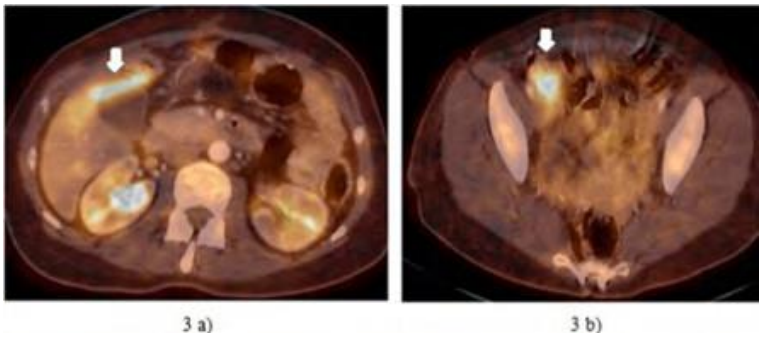

Figure 3a and 2b.

4.4. Pathological Anatomy Definitive

Macroscopic anatomy showed a gastrectomy specimen of 25 cm in the greater curvature and 6 cm in the lesser curvature. After examining the specimen, no visible cancerous lesions in the region where the gastric antrum's serous layer retracted were found. The gastric mucosa appeared flattened and the distinct layers of the gastric wall were indistinguishable. The microscopic anatomy showed a signet ring cell GC-PCC with a G-3 degree of differentiation. The tumor extended through the gastric wall and duodenum and infiltrated the fat of the transverse colon and the greater omentum. Carcinoma infiltrated the distal duodenal resection margin. The number of affected nodes was 4/13. The definitive tumor stage was pT4b pN2. The patient in case 4 has been previously diagnosed and treated at other centers and came to us for a second medical opinion. The tissue used for immunohistochemistry and sequencing came from the endoscopic biopsies performed for the initial diagnosis.

4.5. Sequencing

Next-generation sequencing on gastric tumor tissue was performed to evaluate potential therapeutic targets. The gene variant symbol identified in signet ring type GC-PCC tissue was CREBBP. The synonym of this gene is histone lysine acetyltransferase CREBBP, CHEMBL5747 (ChEMBL), and the protein transcribed by the CREBBP gene, NM004380.3, corresponds to Q92793

CBP_Human (UniprotKB), whose name is CREB-binding protein (Gene Ontology). In the tumor, the CREBBP variant c.5320C>T, p. (Arg1774Cys) was identified in 5% of the mapped sequences (read depth 877x), resulting in the substitution of an arginine for a cysteine at position 1774 of the p. (Arg1774Cys) protein. The dbSNP, ClinVar, or Cosmic databases do not record this variant. In addition, the TP53 c.375G>A variant p. (Thr125=) has been identified in 6% of the sequences mapped in that region of the gene (read depth 1740 x), which does not modify the amino acid at position 125 of the protein: p. (Thr125=). The TP53 c.375G>A variant is not expected to produce an amino acid change (p. =). This variant has been registered in the dbSNP database (rs55863639), categorized in the database (ClinVar/Ds ClinVar: 177825) as a pathogenic or probably pathogenic variant and registered in COSMIC (COSV53120615), associated with tumors of the upper aero/digestive tract and stomach among others. The mutational load was low and there was microsatellite stability (Table 1) (Appendix 2).

Table 1: Case 4. GC-PCC of signet ring cells, located in the antrum and duodenum.

Paraffin samples. Tumor infiltration 70%. NGS panel of 500 genes.				
Transcribed genes for the identification of biomarkers with prognostic and predictive value for response.			Mutational loading	MSI
			2 Mut/Mb^{+} Down load	Microsatellite stability
NM_004380.3	CREBBP	c.5320C>T; p.(Arg1774Cys		
NM_00046.6	TP53	c.375G>A p.(Thr 125=)		

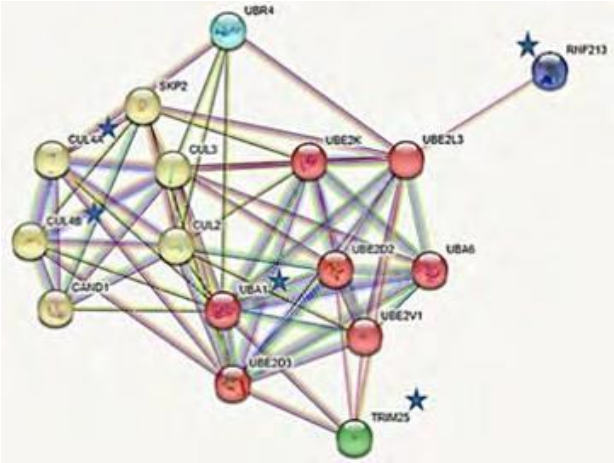

Figure 4

4.6. Oncologic History of Cases 1, 2 and 3

In order to analyze the data regarding the quantification values of the proteins expressed by the genes observed in the sequencing of case 4, three patients with three histopathological subtypes of GC-PCC were selected of a doctoral thesis project of our research group, two males and one female, aged 67, 86 and 73 years, defended in 2021. Case 1 showed a large number of intestinal-like tumor cells with little mesenchymal reaction, no signet ring cells and no necrosis. The tumor was located in the gastric body with lymphatic diffusion, high tumor burden and peritoneal dissemination. Case 2 was a signet ring cell GC-PCC. The tumor was located in the gastric body, with lymphatic diffusion, high tumor burden and peritoneal dissemination. Finally, case 3 was a not specified GC-PCC, located in the gastric antrum, with necrosis and scarce signet ring cells and peritoneal dissemination in the form of plastic linitis gastric, (Table 2) (Appendix 2).

Table 2: GC-PCC. Zorrotzaurre Clinic (case 4) (Sequencing analysis).

Clinical data	Case 4 Tumor 4 /Healthy 4	Case 1 Tumor 1/ Healthy 1	Case 2 Tumor 2/ Healthy 2	Case 3 Tumor 3/ Healthy 3
Age /years	44	73	67	86
Sex	Woman	Man	Man	Woman
AP	Poorly cohesive gastric and duodenal carcinoma (PCC-GC)	Diffuse gastric carcinoma	Poorly Cohesive Gastric Carcinoma (PCC-GC)	Gastric carcinoma poorly cohesive carcinoma not otherwise specified (PCC-NOS)
Cytology	Signet ring cells	Intestinal tumor like	Signet ring cells	Plastic linitis gastric
Location	anthro	body	body	anthro
TNM	cT3N0	T3N2 (3+/16)	T4 N3a (33+/41)	T3N2 (+3/20)
	1º Gatrojejunostomy			
	2º Gastrectomy 2/3, distal duodenectomy. Lymphadenectomy D2 Duodenal exclusion. Gastrojejunostomy		Laparoscopic Subtotal gastrectomy Lymphadenectomy D1+	Subtotal gastrectomy. Lymphadenectomy D2
Surgery	in Y Roux	Subtotal gastrectomy Lymphadenectomy D1+		
Survival	5 months	5 years disease-free	6 months	8 months
			Peritoneal carcinomatosis. Death	Peritoneal carcinomatosis. Death
Live or Die	Live	Lung neoplasm. Death		
Chemotherapy	Trastuzumab and Folfox	LV-5FU	without treatment	without treatment

Hospital Cruces (Cases 1, 2, 3) (Proteomic analysis).

5. Material and Methods

5.1. GC-CCP. Cases 1, 2, 3. Analysis Proteomic

The sample came from gastric tissues obtained after surgery. For the analysis six gastric tissue samples has been used, three tumors and three healthy ones distant from the tumor. The liquid chromatography-mass spectrometry (LC-MS) was use for proteomic analysis. The results obtained correspond to the quantification values of the TU/SA ratio of each protein. Statistical analysis was carried out using XLSTAT software. Several variables, including three histopathological tumor subtypes (categorical variables), the quantitative values of the tumor/health ratio (TU/SA), and the identified proteins and the identifiers (IDs) of the genes encoding these proteins (qualitative variables) were calculated. The event values of the TU/SA ratio of these proteins (=1or >1or <1), obtained from the quantification values, were also added. Values of the TU/SA ratio equal to or greater than 1 indicate, that the protein calculated has a higher quantification in tumor tissue, while if the value of this ratio is less than 1, the protein of interest is higher in healthy tissue. Using supervised automated learning (K-means) proteins were grouped and matched to the different histopathological subtypes of GC-CCP. In addition, Gene Ontology performed functional enrichment of genes and String protein-protein communication. Finally, sensitivity and specificity, precision and area under the curve for each protein were calculated.

6. Results

In the sequencing of case 4, it was identified a mutation in the CREBBP gene, involving an amino acid change from Arginine to Cysteine. Therefore, the quantification value of the TU/SA ratio of the proteins Q92793 CBP, including (O00560 SDCBP) and (Q09161 NCBP1), as well as the proteins related to the amino acids Arginine and Cysteine, was calculated in the three subtypes of CG-PCCs (C1, C2 and C3).

In addition, for tumor protein (Q53FA7 TP53I3, inducible protein p53 3) it has been calculated the quantification value of the TU/SA ratio. The PIG3 gene encodes inducible protein p53 3. This protein is similar to oxidoreductases, enzymes involved in cellular reactions to oxidative stress and radiation exposure. The tumor suppressor protein, p53, is involved in cell division arrest, DNA repair and apoptosis.

6.1. Quantification Values of the TU/SA Ratio of SDCBP and NCBP1, TP53I3 Proteins in The Three GC-PCC Subtypes

(Appendix 2) contains the Panther document, in which Table 3 details the molecular characteristics of these proteins. Table 4 shows the quantification values of the TU/SA ratio for these proteins together with the event values.

6.2. Sensitivity and Specificity Analysis of SDCBP, NCBP1 and TP53I3 Proteins

In intestinal like GC-PCC, the highest sensitivity plus specificity and accuracy is for the protein (O00560 SCDBP), with a value of 2 and 1 respectively; however, in signet ring and not specified cell GC-PCC, this sensitivity, specificity and accuracy is for the protein (Q09161 NCBP1), Tables 5 (a), (b) and (c). The ROC analysis of these proteins in the three GC-PCC tumor subtypes have an area under the curve of one, (Appendix 2). The NCBP1 gene plays an important role in the regulation of RNA transcription and stability. Its protein is involved in signaling pathways that promote proliferation, apoptosis evasion and cell migration. Given its high molecular specificity, it´s use as biomarker in this disease may contribute to improve its diagnosis and treatment.

6.3. Quantification Values of the TU/SA Ratio of SDCBP and Proteins Related to the Amino Acids Arginine and Cysteine in the three GC-PCC Subtypes

In the CG-PCCs of cases 1, 2 and 3, characteristics of the proteins associated with arginine- and cysteine were taken from Panther database, Table 6. Table 7 (Appendix 2) shows the values quantifying the TU/SA ratio and the event values related to these proteins.

Table 3: SDCBP, NCBP1 and TP 53I3 proteins in cases 1, 2 and 3. Analysis in Panther**.**

Gene ID	Mapped IDs	Gene Name	Panther family/ subfamily	Panther protein class	Species
HUMAN|HGNC=10662|UniProtKB=O00560	SDCBP	Syntenin-1 SDCBP PTN002487632 orthologs	Syntenin-1 (pthr12345:sf10)	membrane trafficking regulatory protein	Homo sapiens
HUMAN|HGNC=7658|UniProtKB=Q09161	NCBP1	Nuclear cap-binding protein subunit 1 NCBP1 PTN002488067 orthologs	Nuclear cap-binding protein subunit 1 (pthr12412:sf2)	RNA splicing factor	Homo sapiens
HUMAN|HGNC=19373|UniProtKB=Q53FA7	TP53I3	Quinone oxidoreductase PIG3 TP53I3 PTN002534289 orthologs	Quinone oxidoreductase pig3 (pthr48106:sf18)	oxidoreductase	Homo sapiens

Table 4. CG-PCC: Intestinal like, signet ring and not specified. Values quantification TU/SA ratio and event values SDCBP, NCBP1, TP53I3 proteins.

Majority protein Ids	Protein names	Gene names	CG-PCC intestinal like Case H.Cruces 1 Tumor1/ Health1	1 Value event 1_0	CG-PCC signet ring cells Case Cruces 2 Tumor2/Health2	2 Value event 1_0	CG-PCC Not specified Case H.Cruces 3 Tumor 3/Sano3	3 Value event 1_0
O00560-3; O00560; G5EA09; O00560-2	Syntenin-1	SDCBP	1,001890	1	1,082564	1	1,053924	1
Q09161	Nuclear cap-binding protein subunit 1	NCBP1	1,108420	1	1,080430	1	1,023469	1
Q53FA7	Quinone oxidoreductase PIG3	TP53I3	0,980584	0	1,050681	1	1,019911	1

Table 5: GC-CCP: a) Intestinal like, b) Signet ring cells c) Not specified. SDCBP, NCBP1 and TP53 proteins. Analysis ROC.

5 a) ROC Analysis (Case H. Cruces 1, Tumor 1/ Healthy 1)			
Protein ID	Case H. Cruces 1 Quantification Values Tumor 1/ Healthy 1	Sensitivity+ Specificity	Accuracy
TP53I3	0,980584	1	0,666666
SDCBP	**1,001889**	**2**	**1**
NCBP1	1,108420	1,5	0,666666
The test is positive if Case H. Cruces 1, Tumor 1/Healthy 1 >= the threshold value.			

5 b) ROC analysis (Case H. Cruces 2, Tumor 2/ Healthy 2)			
Protein ID	Case H. Cruces 2 Quantification Values Tumor 2/ Healthy 2	Sensitivity+ Specificity	Accuracy
TP53I3	1,050681	1	0,666667
NCBP1	**1,080430**	**2**	**1,000000**
SDCBP	1,082564	1,5	0,666667
The test is positive if Case H. Cruces 2, Tumor 2/ Healthy 2 >= the threshold value.			

5 c) ROC Analysis (Case H. Cruces 3, Tumor 3/ Healthy 3)			
Protein ID	Case H. Cruces 3 Quantification Values Tumor 3/Healthy 3	Sensitivity+ Specificity	Accuracy
TP53I3	1,019910522	1	0,666666
NCBP1	**1,023469266**	**2**	**1**
SDCBP	1,053923558	1,5	0,666666
The test is positive if Case H. Cruces 3, Tumor 3/Health 3 >= at threshold value			

Table 6: CG-PCC cases 1, 2 and 3, Genes and proteins related to the amino acids Arginine and Cysteine, identified in the Panther database.

UniprotKB access code	Gene ID	Gene Name	PANTHER Family/ Subfamily	PANTHER Protein Class
HUMAN|HGNC=30239 |UniProtKB= Q9H1C7	CYSTM1	Cysteine-rich and transmembrane domain-containing protein 1	Cysteine-rich and transmembrane domain-containing protein 1 (pthr47564:sf1)	-
HUMAN|HGNC=1493| UniProtKB= P49589	CARS	Cysteine--tRNA ligase, cytoplasmic	Cysteine--tRNA ligase, cytoplasmic (pthr10890:sf3)	Aminoacyl-tRNA synthetase
HUMAN|HGNC=2360| UniProtKB= P50238	CRIP1	Cysteine-rich protein 1	Cysteine-rich protein 1 (pthr46074:sf3)	Actin or actin-binding cytoskeletal protein
HUMAN|HGNC=10662| UniProtKB=O00560	SDCBP	Syntenin-1	Syntenin-1 (pthr12345:sf10)	Membrane trafficking regulatory protein
HUMAN|HGNC=5187 |UniProtKB= Q99873	PRMT1	Protein arginine N-methyltransferase 1	Protein arginine n-methyltransferase 1 (pthr11006:sf54)	Protein modifying enzyme

HUMAN|HGNC=9870 |UniProtKB= P54136	NFS1	Cysteine desulfurase	PTN002480847	Fe-S groups DNA synthesis, DNA repair DNA metabolic functions
HUMAN|HGNC=9870 |UniProtKB= P54136	RARS	Arginine--tRNA ligase, cytoplasmic	Arginine--tRNA ligase, cytoplasmic (pthr11956:sf5)	Aminoacyl-tRNA synthetase
HUMAN|HGNC=7658| UniProtKB= Q09161	NCBP1	Nuclear cap-binding protein subunit 1	Nuclear cap-binding protein subunit 1 (pthr12412:sf2)	RNA splicing factor
HUMAN|HGNC=7059 |UniProtKB= P16455	MGMT	Methylated-DNA--protein-cysteine methyltransferase	Methylated-DNA--protein-cysteine methyltransferase (pthr46460:sf1)	-
HUMAN|HGNC=2361| UniProtKB= P52943	CRIP2	Cysteine-rich protein 2	Cysteine-rich protein 2 (pthr46074:sf2)	Actin or actin-binding cytoskeletal protein
HUMAN|HGNC=758| UniProtKB= P00966	ASS1	Argininosuccinate synthase	Argininosuccinate synthase (pthr11587:sf5)	Ligase
HUMAN|HGNC=10648|UniProtKB=Q129	AIMP1	Aminoacyl tRNA synthase complex-interacting multifunctional protein 1	Aminoacyl tRNA synthase complex-interacting multifunctional protein 1 (pthr11586:sf33	Translational protein

Table 7. Histopathological type of PCC of cases H Cruces 01, 02, 03, subtypes, intestinal like, signet ring cell and not specified. Quantification values of the TU/SA ratio and event values, and those related to the amino acids Arginine _Cysteine.

Gene names	ID Gene	CG-PCC intestinal like Case Cruces 1 Tumor 1/ Health 1	CG-PCC intestinal like Value event Tumor 1/ Health 1	GC-PCC signet ring cells Case Cruces 2 Tumor 2 / Health 2	GC-PCC signet ring cells Value event Tumor 2/ Health 2	GC-PCC Not specified Case Cruces 3 Tumor 3/ Health 3	GC-PCC Not specified Value event Tumor 3/ Health 3
Cysteine--tRNA ligase, cytoplasmic	CARS	1,005945	1	0,980259	0	1,007453	1
Methylated-DNA--protein-cysteine methyltransferase	MGMT	1,008253	1	1,086655	1	1,006932	1
Cysteine-rich protein 1	CRIP1	1,066226	1	0,989837	0	1,159598	1
Cysteine-rich protein 2	CRIP2	1,011334	1	0,948087	0	1,092445	1
Cysteine-rich and transmembrane domain-containing protein 1	CYSTM1	0,952692	0	1,075663	1	0,963482	0
Cysteine desulfurase, mitochondrial	NFS1	0,955891	0	0,996317	0	0,872603	0
Protein arginine N-methyltransferase 1	PRMT1	1,004222	1	1,050996	1	1,010979	1
Arginine--tRNA ligase, cytoplasmic	RARS	0,985259	0	1,050130	1	0,998621	0

Syntenin-1	SDCBP	1,082564	1	1,053924	1	1,001890	1
Nuclear cap-binding protein subunit 1	NCBP1	1,108420	1	1,080430	1	1,023469	1
Aminoacyl tRNA synthase complex-interacting multifunctional protein1; Endothelial monocyte-activating polypeptide 2	AIMP1	0,948271	0	1,073355	1	1,004567	1
Argininosuccinate synthase	ASS1	0,935199	0	0,958318	0	0,947429	0

6.4. Differential Expression of Proteins Related to the Amino Acids Arginine and Cysteine

In GC-PCCs of the intestinal like and not specified types, the ratios between tumor and healthy tissue (TU/SA) for the proteins cytoplasmic t RNA cysteine ligase (P49589 CARS) and cysteine-rich protein 1 (P50238 CRIP1) exceed the value of 1. This indicates that the presence of these proteins is higher in tumor tissue compared to healthy tissue. On the other hand, in CG-PCC signet ring cell cancer, these quantifications are higher in healthy tissue than in tumor tissue, as detailed in table 7 in (Appendix 2). Significant differences were observed in the differential expression of the TU/SA ratio of event values of CARS and CRIP1 proteins, in the CG-PCC, intestinal like type, Table 8 a. Likewise, in the CG-PCC of signet ring cells, these differences are significant for the protein (P16455 MGMT DNA methylated-protein cysteine methyl transferase), Table 8 b). In all three GC-PCC subtypes, the MGMT protein is more highly expressed in tumor than in healthy tissue, table 7 (Appendix 1). This protein is involved in DNA repair by removing methyl groups added to the molecules. These tumors with high levels of this protein have higher levels of genomic damage due to their rapid proliferation and a microenvironment with inflammation and hypoxia. Elevated levels of MGMT allow cells to cope more effectively with genomic damage, potentially increasing their survival and progression. Finally, in the not specified CG-PCC case, CARS and CRIP1 proteins show significant differential expression between tumor and healthy tissue, Table 8 c) (Appendix 2). We have also calculated the differential expression of the quantification values of the TU/SA ratio of the multifunctional protein one, which interacts with protein complex (Q12904 AIMP1 Aminoacyl RNA synthase complex-interacting multifunctional protein 1) and (ASS1 Arginino-succinate synthase). In the GC-PCC, the P00966 ASS1 protein has values lower than one, which means that the quantification values are higher in healthy tissue, (Table 7) (Appendix 2). In signet ring GC-PCC the protein (P54136 RARS Arginine-cytoplasmic t RNA ligase) shows a higher TU/SA ratio of quantification values in the tumor, with a significant differential expression between tumor and healthy tissue, with a p-value <0.001, table 9 (appendix 2). An increase in the TU/SA ratio of RARs protein levels in cancer tissue was detected in the study of CG-PCC signet ring cell. The increase may be associated with an adverse prognosis for patients, all of them in tumor stage III-IV.

6.5. Acetylation of SDCBP and NCBP1, Histone Acetyltransferase type B Catalytic Subunit (HAT) and Histone Deacetylases (HDAC) Proteins

Histone acetylation and Histone deacetylase are epigenetic processes involved in the regulation of gene expression, acting on chromatin conformation. The regulation occurs by the opposing action of two enzymes: histone lysine acetyltransferase (HAT) and histone deacetylase (HDAC).This deacetylase boosts the loss of the acetyl group at the amino-terminal tail of histones, leading to chromatin condensation and repression of gene transcription. The characteristics of proteins (O00560 SDCBP) and (Q09161 NCBP1) and Histones (Q13547 HDAC1), have been analyzed in the Panther database (Table 10) (Appendix 2). The quantification values and event values of these proteins for the three GC-PCC subtypes are in (Table 11) (Appendix 2). The quantification value of the TU/SA ratio of the proteins (O00560 SDCBP and Q09161NCBP) and (Q13547 HDAC1 Histone deacetylase 1), are higher in tumor than in healthy tissue in all three GC-CCP subtypes. The proteins (O00560 SDCBP) of intestinal CG-PCC like show differential expression, with a significant p value in tumor, relative to healthy tissue, (Table 12) (Appendix 2). On the other hand, (Q13547 HDAC) has a significantly higher differential expression in healthy tissue than in tumor. In CG-PCC of signet ring and not specified cells, there are no significant differences for these proteins between tumor and healthy tissue.

Table 8 a). GC-PCC intestinal like	**Results for the factor event.**			**Value Tumor 1/Health 1**
3 traits with the lowest p-values				
Features	p-value	Significant	0	1
CARS	**0,007**	**Yes**	0,955 (b)	1,041 (a)
CRIP1	**0,043**	**Yes**	0,957 (b)	1,043 (a)
MGMT	0,910	No	1,031 (a)	1,027 (a)

Table 8 b). GC-PCC signet ring cells	**Results for the factor event.**			**Value Tumor 2 /Health 2**
3 traits with the lowest p-values				
Features	p-value	Significant	0	1
MGMT	**<0,0001**	**Yes**	0,975 (b)	1,066 (a)
CARS	0,632	No	0,995 (a)	1,024 (a)
CRIP1	0,756	No	1,016 (a)	1,001 (a)

Table 8 c). GC-PCC Not specified	**Results for the factor event**			**Value Tumor 3 /Health 3**
3 traits with the lowest p-values				
Features	p-value	Significant	0	1
CARS	**0,019**	**Yes**	0,957 (b)	1,041 (a)
CRIP1	**0,037**	**Yes**	0,946 (b)	1,043 (a)
MGMT	0,838	No	1,02 (a)	1,027 (a)

Table 9: GC-CCP intestinal like, signet ring cells and not specified. Value p significant of the TU/SA ratio AIMP1, ASS1 and RARs proteins.

Tumor	Proteins	TU/SA Value p
CG-PCC intestinal like	AIMP1	0,002
	ASS1	0,025
CG-PCC signet ring cells	RARS	<0,001
CG- PCC not specified	ASS1	0,032

Table 10: Characteristics of SDCBP, NCBP1 and Histone proteins from the Panther* database. IDs, with unique mapping.

Gene ID	**Mapped Ids**	**Gene Name**	**Panther family/ subfamily**	**Panther Protein Class**
		Gene Symbol		
	HIST1H4A	Histone H4	Histone h4 (pthr10484:sf210)	Chromatin/ chromatin-binding, or -regulatory protein
HUMAN|HGNC=20510|UniProtKB=P62805		H4C16		
		PTN002470965		
		orthologs		

	SDCBP	Syntenin-1	Syntenin-1 (pthr12345:sf10)	Membrane trafficking regulatory protein
HUMAN|HGNC=10662|UniProtKB=O00560		SDCBP		
		PTN002487632		
		orthologs		
	HDAC1	Histone deacetylase 1	Histone deacetylase 1 (pthr10625:sf49)	-
HUMAN|HGNC=4852|UniProtKB=Q13547		HDAC1		
		PTN002472122		
		orthologs		
	RBBP4	Histone-binding protein RBBP4	Histone-binding protein RBBP 4 (pthr22850:sf90)	-
HUMAN|HGNC=9887|UniProtKB=Q09028		RBBP4		
		PTN002504663		
		orthologs		
	NCBP1	Nuclear cap-binding protein subunit 1	Nuclear cap-binding protein subunit 1 (pthr12412:sf2)	RNA splicing factor
HUMAN|HGNC=7658|UniProtKB=Q09161		NCBP1		
		PTN002488067		
		orthologs		

*Proteins not listed in the table, identified as unassigned in Panther.

Table 11. Quantification and event values for CBP and histone proteins in the three GC-CCP subtypes.

Majority protein Ids	Protein names	Gene names	Tumor 1/Sano 1 GC-PCC Intestinal like	GC-PCC Intestinal like. Valores evento precoz 0 / tardío 1	GC-PCC células en anillo de sello Tumor 2/Sano 2	CG-PCC célula anillo de sello. Valores evento precoz 0 / tardío 1	CG-PCC no especificado Tumor 3/Sano 3	GC PCC no especificado. Valores evento precoz 0 / tardío 1
O00560-3; O00560; G5EA09; O00560-2	Syntenin-1	SDCBP	1,001889956	1	1,082564223	1	1,053923558	1
Q09161	Nuclear cap-binding protein subunit 1	NCBP1	1,108420124	1	1,080430253	1	1,023469266	1
Q13547; Q5TEE2	Histone deacetylase 1	HDAC1	1,026164675	1	1,173105143	1	1,030947374	1
P68431	Histone H3.1	HIST1H3A	0,87294918	0	1,114221514	1	1,224701476	1
Q5TEC6	Histone H3	HIST2H3PS2	1,012030053	1	1,008456142	1	0,99512941	0
K7EX07; P84243; K7EMV3; B4DEB1; K7ES00; Q16695; K7EP01; Q6NXT2	Histone H3;Histone H3.3;Histone H3.1t;Histone H3.3C	H3F3B;H3F3A;HIST3H3;H3F3C	1,040941134	1	1,023926968	1	1,023028789	1
O75367-3;O75367; O75367-2; B4DJC3	Core histone macro-H2A.1;Histone H2A	H2AFY	1,006672232	1	1,055263557	1	1,022672391	1
P07305-2;P07305	Histone H1.0;Histone H1.0, N-terminally processed	H1F0	1,057836595	1	0,983461827	0	1,024367979	1
P16401	Histone H1.5	HIST1H1B	1,030673566	1	1,083800893	1	1,043939897	1
P16403	Histone H1.2	HIST1H1C	0,99532365	0	1,025107917	1	1,024243834	1
P62805	Histone H4	HIST1H4A	1,003115371	1	1,045863087	1	1,018935076	1
P68431	Histone H3.1	HIST1H3A	0,87294918	0	1,114221514	1	1,224701476	1
Q09028-3;Q09028; Q09028-4; Q09028-2	Histone-binding protein RBBP4	RBBP4	1,020546196	1	1,038397036	1	1,027152533	1
Q92522	Histone H1x	H1FX	1,004667658	1	0,980471601	0	1,0542884	1
Q99878; Q96KK5; Q6STM1; Q16777; Q93077; Q7L7L0; Q6FI13; P20671; P0C0S8; P04908; B0YFX9	Histone H2A type 1J; Histone H2A type 1-B; Histone H2A J; Histone H2A type 2-C; Histone H2A type 1-C; Histone H2A type 3; Histone H2A type 2-A; Histone H2A type 1-D; Histone H2A type 1; Histone H2A type 1-B/E; Histone H2A	HIST1H2AJ; HIST1H2AH; H2AFJ; HIST2H2AC; HIST1H2AC; HIST3H2A; HIST2H2AA3; HIST1H2AD; HIST1H2AG; HIST1H2AB	0,964655149	0	1,034094753	1	1,033063073	1
U3KQK0; Q99880; Q99879; Q99877; Q93079; Q5QNW6; P62807; P58876; P57053; O60814; Q5QNW6-2	Histone H2B; Histone H2B type 1-L; Histone H2B type 1-M; Histone H2B type 1-N; Histone H2B type 1-H; Histone H2B type 2-F; Histone H2B type 1-C/E/F/G/I; Histone H2B type 1-D; Histone H2B type F-S; Histone H2B type 1-K	HIST1H2BN; HIST1H2BL; HIST1H2BM; HIST1H2BH; HIST2H2BF; HIST1H2BC; HIST1H2BD; H2BFS; HIST1H2BK	0,977953905	0	1,064868436	1	1,009141458	1

Table 12: GC-PCC Intestinal like. Results for the event factor. Values early event 0 / late event 1.

three traits with the lowest p-values				
Features	valor-p	Significativo	0	1
SDCBP	**0,003**	**Sí**	0,926 (b)	**1,028 (a)**
HDAC1	**0,016**	**Sí**	**1,127 (a)**	1,029 (b)
NCBP1	0,506	No	1,072 (a)	1,051 (a)

6.6. Proteins (O00560 SDCBP), (P62805 HIST1H4A), (Q13547 HDAC1): Sensitivity Plus Specificity and Accuracy. AUC

The quantification of the TU/SA ratio of the protein (O00560 SDCBP) in the tumor, together with its high sensitivity, specificity, accuracy and area under the curve, Table 13 (Appendix 2), reflect its importance in intestinal-like GC-CCP. This protein contributes to invasion, resistance to apoptosis and adaptation to the tumor environment. These features highlight the potential of the protein (O00560 SDCBP) as a prognostic biomarker and therapeutic target. The protein (Q13547 HDAC1) is crucial for chromatin structure and various post-translational modifications can affect it. In CG-PCC of signet ring cells, the sensitivity and specificity of this protein reaches an index of 1.091, while its accuracy is 0.375, with an AUC of 0.364. Thus, (Q13547 HDAC1) could reinforce chromatin condensation in this cell type, blocking transcription. The quantification, sensitivity, specificity, precision and AUC values for the protein (P62805 HIST1H4A) in the not specified GC-PCC in Table 13 (Appendix 2), are detailed.

6.7. Ubiquitin Ins

The ubiquitin-proteasome system (UPS) is a main pathway for protein degradation in mammals. This system regulates cellular processes such as signal transduction, cell cycle, transcription, DNA damage and repair.

The ubiquitin characteristics described were checked in Panther database, (Table 14 (a-b) (Appendix 2). The quantification values of the TU/SA ratio of the ubiquitin system proteins and the event values (early or late phase) can be seen in Table 15 (Appendix 2) and come from the proteomic analysis of cases C1, C2 and C3. The Table 16 in (Appendix 2) presents the results of the hierarchical agglomerative clustering of ubiquitin proteins performed using the K-means method. Cluster three consisting of proteins (P22314 UBA1), (Q14258 TRIM25) and (Q13619 CUL4A) and (Q13620 CUL4B) is the most homogeneous, having the lowest within-cluster variance and the highest silhouette score. In all three CG-PCC subtypes, the proteins with the TU/SA ratio of quantification values above one were (Q14258 E3 ubiquitin/ISG15 ligase), (Q14258 TRIM25), (Q13619 CUL4A) and (Q13620 CUL4B), indicating a higher presence of these proteins in the tumor. However, in the case of (P22314 UBA1) the ratio of the quantification values of this protein in the not specified GC-PCC are less than one, indicating a higher presence in healthy tissue. The String analysis shows the association networks of the functional proteins related to ubiquitin in the CG-PCC. Node one controlled by the protein (P22314 UBA1) is marked with a star. This node is formed by seven genes marked in red composed of different isoforms of ubiquitin. Six genes marked in yellow form node 2. The genes (P22314 UBE1) and (P61086 UBE2K) are the controllers of the different isoforms of CULLIN and (Q13309 SKP2), which are involved in the G1/S transition of the mitotic cell cycle and of neddylation domain of the CULLIN protein. Q14258 (TRIM25) is part of cluster three, and its activity is associated with the proteins P61077 (UBE2D3) and Q13404 (UBE2V1). UBRA4 is categorized within cluster 4, and the RNF213 protein is connected to UBE2L3 (Figure 4, Appendix 1).

Table 13: GC-CCP subtypes. CBP genes and Histones. Sensitivity plus specificity. Accuracy and AUC.

Type of CG-CBP	Gene ID	Quantification value TU/SA ratio	Sensitivity + specificity	Accuracy	AUC
Intestinal like	SCDB	1,001899	2	1	1
Signet ring cells	HDAC1	1,173105	1,091	0,375	0,364
Not specified	HIST1H4A	1,003115	1,109	0,688	0,345

Table 14 a): Characteristics of Ubiquitin proteins. Panther database.

Gene ID		Gene Name	PANTHER Family/Subfamily	PANTHER Protein Class
HUMAN|HGNC=12494|UniProtKB=Q13404	UBE2V1	Ubiquitin-conjugating enzyme E2 variant 1 UBE2V1 PTN002538180 orthologs	Ubiquitin-conjugating enzyme E2 variant 1 (pthr24068:sf323)	ubiquitin-protein ligase
HUMAN|HGNC=12932|UniProtKB=Q14258	TRIM25	E3 ubiquitin_ISG15 ligase TRIM25 TRIM25 PTN002552051 orthologs	E3 ubiquitin_isg15 ligase TRIM25 (pthr25465:sf77)	ubiquitin-protein ligase

HUMAN|HGNC=2555|UniProtKB=Q13620	CUL4B	Cullin-4B CUL4B PTN002484918 orthologs	Cullin-4b (pthr11932:sf66)	ubiquitin-protein ligase
HUMAN|HGNC=12488|UniProtKB=P68036	UBE2L3	Ubiquitin-conjugating enzyme E2 L3 UBE2L3 PTN002514474 orthologs	Ubiquitin-conjugating enzyme E2l3 (pthr24068:sf67)	ubiquitin-protein ligase
HUMAN|HGNC=12476|UniProtKB=P61077	UBE2D3	Ubiquitin-conjugating enzyme E2 D3 UBE2D3 PTN002514481 orthologs	Ubiquitin-conjugating enzyme E2D3 (pthr24068:sf415)	ubiquitin-protein ligase
HUMAN|HGNC=30313|UniProtKB=Q5T4S7	UBR4	E3 ubiquitin-protein ligase UBR4 UBR4 PTN002502845 orthologs	E3 ubiquitin-protein ligase UBR4 (pthr21725:sf1)	ubiquitin-protein ligase
HUMAN|HGNC=12475|UniProtKB=P62837	UBE2D2	Ubiquitin-conjugating enzyme E2 D2 UBE2D2 PTN002514487 orthologs	Ubiquitin-conjugating enzyme E2 D2 (pthr24068:sf330)	ubiquitin-protein ligase

Tabla 14 b). Características de las proteínas Ubiquitinas.
Base datos Panther (2)

HUMAN|HGNC=2552|UniProtKB=Q13617	CUL2	Cullin-2 CUL2 PTN002484901 orthologs	Cullin-2 (pthr11932:sf174)	ubiquitin-protein ligase
HUMAN|HGNC=2554|UniProtKB=Q13619	CUL4A	Cullin-4A CUL4A PTN002484917 orthologs	Cullin-4a (pthr11932:sf68)	ubiquitin-protein ligase
HUMAN|HGNC=12469|UniProtKB=P22314	UBA1	Ubiquitin-like modifier-activating enzyme 1 UBA1 PTN002475164 orthologs	Ubiquitin-like modifier-activating enzyme 1 (pthr10953:sf155)	ubiquitin-protein ligase

HUMAN|HGNC=2553|UniProtKB=Q13618	CUL3	Cullin-3 CUL3 PTN002484881 orthologs	Cullin-3 (pthr11932:sf168)	ubiquitin-protein ligase
HUMAN|HGNC=14539|UniProtKB=Q63HN8	RNF213	E3 ubiquitin-protein ligase RNF213 RNF213 PTN002503315 orthologs	E3 ubiquitin-protein ligase RNF213 (pthr22605:sf16)	-
HUMAN|HGNC=10901|UniProtKB=Q13309	SKP2	S-phase kinase-associated protein 2 SKP2 PTN002546523 orthologs	S-phase kinase-associated protein 2 (pthr16134:sf32)	ubiquitin-protein ligase
HUMAN|HGNC=4914|UniProtKB=P61086	UBE2K	Ubiquitin-conjugating enzyme E2 K UBE2K PTN002541690 orthologs	Ubiquitin-conjugating enzyme E2 k (pthr24068:sf533)	ubiquitin-protein ligase
HUMAN|HGNC=30688|UniProtKB=Q86VP6	CAND1	Cullin-associated NEDD8-dissociated protein 1 CAND1 PTN002489426 orthologs	Cullin-associated Nedd8-dissociated protein 1 (pthr12696:sf1)	ubiquitin-protein ligase
HUMAN|HGNC=25581|UniProtKB=A0AVT1	UBA6	Ubiquitin-like modifier-activating enzyme 6 UBA6 PTN002475160	Ubiquitin-like modifier-activating enzyme 6 (pthr10953:sf186)	ubiquitin-protein ligase

Table 15: Proteins of the ubiquitin proteasome system. Quantification and event values.

Majority protein Ids	Protein names	Gene names	GC-PCC 1 Intestinal like. Caso Cruces 1. Tumor 1/ Sano 1	GC-PCC1 Intestinal like-Valores evento 0_1	GC-PCC 2 Anillo de sello. Caso Cruces 2. Tumor2/ Sano2	GC-PCC 2 Anillo de sello. Valores evento 0_1	GC-PCC 3 no especificado. Caso Cruces 3. Tumor3/ Sano3	GC-PCC 3. Valores evento 0_1
A0A087WY85; P61077; P61077-2; P61077-3; D6R9F6; D6R933; D6RGD0; D6R980; D6RIZ3; D6RA11; D6RFM0; D6RAH7; H9KV45; A0A0A0MQU3; P62837-2; P62837	Ubiquitin-conjugating enzyme E2 D3;Ubiquitin-conjugating enzyme E2 D2	UBE2D3; UBE2D2	0,992922714	0	0,919773401	0	1,017301253	1
A0A0A0MTR7; A0A0A0MTC1; Q63HN8; Q63HN8-4	E3 ubiquitin-protein ligase RNF213	RNF213	0,962380991	0	0,961848668	0	1,03229552	1
P22314-2;P22314	Ubiquitin-like modifier-activating enzyme 1	UBA1	0,994136076	0	1,019421324	1	1,013990733	1

A0AVT1; A0AVT1-2	Ubiquitin-like modifier-activating enzyme 6	UBA6	1,028059943	1	0,962620875	0	0,98477266	0
I3L0A0; Q13404; Q13404-7; Q13404-2; Q13404-1; G3V2F7; Q13404-8; A0A0A0MSL3; Q13404-6	Ubiquitin-conjugating enzyme E2 variant 1	TMEM189-UBE2V1; UBE2V1	1,007556419	1	0,955548525	0	1,059291485	1
P61086; D6RDM7; P61086-3	Ubiquitin-conjugating enzyme E2 K	UBE2K	1,018705262	1	0,990843518	0	1,000838975	1
P68036-2; P68036; P68036-3; A0A0B4J2G9	Ubiquitin-conjugating enzyme E2 L3	UBE2L3; hCG_1789329	1,008402644	1	0,982140283	0	1,009687346	1
Q5T4S7-3; Q5T4S7-4; Q5T4S7; Q5T4S7-2; Q5T4S7-5; A0A0A0MSW0	E3 ubiquitin-protein ligase UBR4	UBR4	0,997493481	0	0,983073245	0	0,985506236	0
Q14258	E3 ubiquitin/ISG15 ligase TRIM25	TRIM25	1,004222742	1	1,024874455	1	1,027961852	1
A0A0A0MR50; Q13619-2;Q13619; A6NE76	Cullin-4A	CUL4A; CUL4B	1,001472499	1	1,063707306	1	1,017439082	1
A0A0A0MTN0; Q13617; Q13617-2; Q5T2B5	Cullin-2	CUL2	0,97346085	0	0,97423654	0	0,991586245	0
Q13618-2;Q13618; Q13618-3	Cullin-3	CUL3	1,097178937	1	0,947913485	0	1,016897487	0
Q86VP6; Q86VP6-2; A0A0C4DGH5	Cullin-associated NEDD8-dissociated protein 1	CAND1	0,994268024	0	0,991218606	0	1,006038383	1
Q8ND24	RING finger protein 214	SKP2	1,095850021	1	0,978092093	0	0,950568209	0

6.8. Differential Expression of Ubiquitin in the Different GC-CCP Subtypes

The atypical E3 ubiquitin-protein ligase (Q63HN8 RNF213), which can activate the ubiquitination of both proteins and lipids and is involved in various processes such as lipid metabolism, angiogenesis and cell-autonomous immunity. In signet ring cell GC-PCC, a significant difference was observed between tumor and healthy tissue when protein (Q63HN8 RNF213) was quantified, Table 18 (appendix 2). In TCGA, two isoforms of the protein (P22314 UBA1 (Ubiquitin-like modifier activating enzyme 1) have been observed in gastrointestinal cancer, which are present in relatively high frequency, with little variation between different tumor subtypes. It catalyzes the first step in the ubiquitin conjugation to target proteins. In signet ring cell GC-PCCs and in the not specified, the quantification value of (P22314 UBA1) is higher in tumor than in healthy tissue. While the intestinal type like has a higher quantification in healthy tissue than in tumor, (Table 12) (Appendix 2). (P22314 UBA1) tags proteins for degradation by the proteasome, a protein complex responsible for removing damaged, misfolded or unneeded proteins. In addition, it is involved in the control of key cellular processes, such as cell cycle, DNA repair, stress response, intracellular signals and apoptosis. These changes contribute to the development of the GC-PCC. The protein (P22314 UBA1) shows significant differential expression in not specified GC-PCC (Table 19) (Appendix 2). (P62837 UBE2D2) and (P611077 UBE2D3), are enzymes that facilitate the transfer of ubiquitin from the E1 enzyme to specific substrate proteins. In the not specified GC-PCC the differences of these proteins between healthy and tumor tissue are not significant.

Table 16: Results by clúster.

Clase	1	2	3	4	Silhouette scores (class averaged)) Clase Silhouette scores	
Number of objects by cluster	5	4	3	2		
Total Weights	5	4	3	2		
Within-cluster variance	0,002	0,001	0,001	0,003		
Minimum distance to centroid	0,021	0,015	0,014	0,036	Clase 1	-0,047
Average distance to centroid	0,036	0,024	0,020	0,036	Clase 2	0,266
Maximum distance to centroid	0,046	0,038	0,028	0,036	Clase 3	0,475
	UBE2D3; UBE2D2	RNF213	UBA1	CUL3	Clase 4	0,284
	UBA6	UBR4	TRIM25	SKP2	Mean width	0,202
	TMEM189-UBE2V1; UBE2V1	CUL2	CUL4A; CUL4B			
	UBE2K	CAND1				
	UBE2L3; hCG_1789329					

Table 17: GC-PCC 2. Signet ring cells results differential expression of Ubiquitin. Values event 0_1.

Three features with the lowest p-values				
Features	p-value	Significant	0	1
RNF213	0,001	Yes	0,968 (b)	1,036 (a)
UBA1	0,550	No	1,005 (a)	1,02 (a)
UBE2D3; UBE2D2	0,550	No	1,016 (a)	1 (a)

Table 18: GC-PCC 3 not specified. Results of differential expression of Ubiquitin. Values event 0_1.

Three Features traits with the lowest p-values				
Features	p-value	Significant	0	1
UBA1	0,026	Yes	0,986 (b)	1,021 (a)
UBE2D3; UBE2D2	0,094	No	1,038 (a)	0,998 (a)
RNF213	0,318	No	0,969 (a)	0,99 (a)

Table 19: Sensitivity and specificity of Ubiquitin and Cullin proteins and their isoforms in GC-PCC.

Protein ID	CULLIN-4A	Protein ID	TRIM25	Protein ID	CULLIN-4A
GC-CCP 1 Intestinal like. Case Cruces 1. Tumor1/Sano1 Quantification values	1,001,472	CG-PCC 2 Signal ring. Case Cruces 2. Tumor2/ Sano2. Quantification values	1,024,874	GC-SCC 3 not specified. Case Cruces 3. Tumor3/Sano3 Quantification Values	1,017,439
Sensitivity+ Specificity	2	Sensitivity+ Specificity	1,25	Sensitivity+ Specificity	1,2
Accuracy	1	Accuracy	0,57	Accuracy	0,57

6.9. Sensitivity, Specificity, Accuracy and AUC of Ubiquitin System Proteins in the three GC-PCC Subtypes

Proteomic analysis shows the involvement of (Q14258 TRIM25) in intestinal GC-CCP. The ratio of the quantification values of the TU/SA ratio of the (Q14258 TRIM25) protein is higher in tumor than in healthy tissue. The sensitivity and specificity are 1.25 and the precision is 0.57, Table 20 (Appendix 2). In intestinal type GC-CCP the highest sensitivity, specificity and accuracy of all proteins is the protein (Q13619 Cullin-4A). Therefore, it could be used as biomarker. The ROC analysis, which measures the accuracy of the model, shows an area under the curve (AUC) of the Ubiquitin proteins with a value of 1 for the intestinal like CG-PCC, 0.600 for the signet ring cell CG-PCC and 0.450 for the not specified ones.

7. Discussion

7.1. Diagnosing and Treating Case 4

The European Society for Medical Oncology (ESMO) clinical guidelines, adapted by the Pan-Asian Guidelines Adaptation (PAGA), recommend with level of evidence [IIIB] exploratory laparoscopy for GC, that can be resected in stages IB-III; also in candidates for perioperative chemotherapy or at risk of peritoneal metastasis [15]. In case 4, as an initial procedure, a diagnostic laparoscopy with peritoneal lavage and cytology was performed and no metastases were found. This provided a first approximation of the stage of the disease, which helped to plan the peri-operative treatment. The tumor extension study determined a tumor stage [IIA]. Some authors have considered that an inspection of the peritoneal cavity at the time of surgery could be performed, making diagnostic laparoscopy part of the procedure prior to resection. In this patient, between May and August 2024, the successive surgical procedures performed were a gastrojejunostomy, laparotomy for internal hernia with intestinal obstruction, a subtotal gastrectomy with D2 lymphadenectomy and partial resection of the transverse colon. Perioperative chemotherapy is the standard treatment for locally advanced GC, but a significant proportion of patients do not complete treatment due to postoperative complications and prolonged recovery. Case 4, after two cycles of initial perioperative chemotherapy with FLOT, was cancel due to disease progression and underwent a surgery due to a gastroduodenal junction obstruction. Total neo-adjuvant chemotherapy can optimize the complete administration of systemic therapy [20]. However, when neo-adjuvant chemotherapy is used, the patients need to be selected carefully according to the pathologic stage, due to the inaccuracies of clinical-radiologic stage [21]. In case 4 after completion of neo-adjuvant treatment, the final pathologic anatomy obtained after gastric resection subtotal and D2 lymphadenectomy was stage [IVB]. The REGATTA clinical trial established that, in advanced GC with metastases, gastrectomy followed by adjuvant chemotherapy (S-1+cisplatin) did not provide a survival advantage over chemotherapy alone [22]. It follows that in case 4, despite the efforts made, neither surgery nor chemotherapy was able to control tumor progression. From GC stage II (≥pT2), a subset of poorly differentiated cells acquired migratory properties, reaching the layers below the mucosa. As these cells spread diffusely into the submucosal and underlying muscle layers, the tumor outgrew the pyloric area and reached the upper knee of the duodenum. Proteomics has recently clarified the molecular characteristics of duodenal cancer [23]. Therefore, in this patient with tumor extension into the duodenum, it was necessary to consider that the molecular changes in the duodenum might be different from those of the primary tumor and, consequently, different from the treatment. A morphologic feature of case 4 was the close relationship of the tumor to the pancreatic head. After chemotherapy, it was performed a distal gastrectomy and resection of a metastasis in the meso-transverse colon, but the resection was not R0 because the distal resection margin of the duodenum was infiltrated. To improve the oncologic prognosis of T4b GC, that infiltrates the pancreatic head and duodenum, it has been proposed to combine the Whipple technique with distal gastrectomy and D2 lymphadenectomy performed by laparoscopy [24]. Combined resection of locally advanced distal gastric cancer that invades the pancreas and duodenum is controversial because of the high morbidity rate and the uncertainty of the procedure in relation to prognosis. The complications of this surgery are correlated with poor oncological outcomes. The resection in block of duodenum, pancreas and stomach, and the strict prevention of postoperative complications, can improve the long-term survival of patients with advanced gastric cancer involving the pancreaticoduodenal region. Well-differentiated histology and negative resection margin are the most important predictors of prolonged survival [25]. Certain genetic and genomic characteristics can predict response to cancer immunotherapy. These include PD-L1 expression, tumor mutation burden (TMB), and microsatellite repair deficiency, which have been evaluated in clinical trials to determine their influence on responsiveness [26-28]. Of all the characteristics reflected, the patient in case 4 showed a large part of them such as, Helicobacter py. (+) at diagnosis, CREBBP and TP53 gene mutations, low mutational load, positive PD-L1 expression and microsatellite stability. Radical duodenal pancreatic resection after neo-adjuvant chemotherapy plus Trastuzumab is an option for HER2-positive locally advanced GC invading the pancreatic head in the absence of non-curative factors [29]. Pembrolizumab, a PD-L1 inhibitor, improved progression-free survival when used with Trastuzumab and chemotherapy compared with placebo, especially in patients with HER2-positive metastatic gastric cancer and an anti-PD-L1 antibody test score of 1 or higher [30]. Mutations of some important oncogenes and tumor suppressor genes are associated with immune signatures in GC, including TP53 [31]. In addition, the tumor immune microenvironment play a crucial role in determining the response to cancer immunotherapy [32]. Case 4, was treated with neo-adjuvant chemotherapy and

Trastuzumab and it was not considered appropriate to add anti PD-L1. Duodenal-pancreatic resection was not performed either, due to the extension of the tumor.

7.2. Analysis of Proteins Related to Mutations in Case 4 and Cases 1, 2, 3, in the three Subtypes of GC-CCP

The development of GC-PCC is a process that involves the interaction of genetic, epigenetic and micro-environmental alterations, resulting in an aggressive cancer with distinctive characteristics in its growth and spread. Since a CREBBP gene mutation was identified in case 4, with an Arginine_Cysteine variation, the proteomic analysis of cases 1, 2 and 3 targeted the following proteins: (Q92793 CBP, as O00560 SDCBP and Q09161 NCBP1) and proteins related to the amino acids arginine (Q99873 PRMT1, P54136 RARS, P00966 ASS1, and Q12904 AIMP1) and cysteine (Q9H1C7 CYSTM1, P49589 CARS, P50238 CRIP1, Q9Y697 NFS1, P16455 MGMT, and P52943 CRIP2). CREBBP gene-binding protein (Q92793 CBP) is a multifunctional protein that regulates the expression of many genes that interact with transcription factors and remodel chromatin through its histone acetyl transferase (HAT) activity. Syntenin 1 protein (O00560 SDCBP), binds to syndecans associated with cytoplasmic proteins. Syntenin is involved in intracellular signaling, cell adhesion, and regulation of migration and metastasis. Nuclear cap-binding protein subunit 1 (Q09161 NCBP1), or (CBP80), is involved in RNA processing and regulation. It is involved in how genes are expressed and how cells respond to cellular stress and DNA damage. Negative regulation of SDCBP inhibits cell proliferation and induces apoptosis by regulating the PI3K/AKT/mTOR pathway in GC33. Nucleosome binding protein 1 (NCBP1) promotes GC cell growth [34]. In all CG-PCC subtypes of cases 1, 2 and 3, SDCBP and NCBP1 proteins have higher TU/SA ratio values in tumor than in healthy tissue. The increase of this protein in all three CG-PCC subtypes could facilitate cell proliferation and inhibit apoptosis, which would facilitate migration and metastasis. In case 4 with mutation of the CREBBP gene, the proteins (Q92793 CBP) could have maintained cell proliferative activity, in a similar way as they did in cases 1, 2 and 3, in which we do not know whether or not they had this same mutation. It is possible that in case 4 the SDCBP protein participated in the cellular response to DNA damage, while NCBP, being a protein that regulates messenger RNA, could have been essential to ensure that the repair genes were expressed efficiently. Protein arginine N-methyl-transferase 1 (Q99873 PRMT1) PRMT1 promotes gastric cancer cell proliferation and metastasis by recruiting MLXIP for transcriptional activation of the β-catenin pathway [35]. Arginine-tRNA ligase cytoplasmic (P54136 SYRC) (RARS gene) is part of a macromolecular complex, which catalyzes the binding of specific amino acids to cognate tRNAs during protein synthesis. It was observed that the protein (P16455 MGMT), a cysteine methyltransferase that repairs methylated DNA bases by transferring the methyl group to a cysteine residue in the enzyme itself, could be involved in the early stages of methylation in this type of cancer. These methylation events produced by the protein (P16455 MGMT) could cause changes in DNA that influence CYSTM1 protein expression, keeping its levels elevated compared to other cysteines in the tumor. Finally, the protein cysteine methyl-transferase (P16455 MGMT) is a protein for the identification and repair of damaged DNA in gastric mucosal epithelial cells and loss of its gene expression can lead to the development of gastric cancer [36]. This protein is epigenetically regulated, mainly by methylation of the MGMT promoter [37]. It removes harmful methyl groups from guanine in DNA, which prevents mutations that could lead to cancer. Arginino-succinate synthetase 1 (P00966 ASS1) contributes to gastric cancer invasion and progression by modulating autophagy [38]. In case 2 all the arginines analyzed are more abundant in the tumor than in healthy tissue, except for the protein Argininosuccinate synthase (P00966 ASS1). This protein is responsible for arginine biosynthesis in most body tissues. This could be the reason why, with decreased levels of Arginine in the tumor, tumor cells become dependent on exogenous arginine instead of synthesizing it by the tumor. Likewise, epigenetic mechanisms such as methylation of the ASS1 gene promoter in tumor cells could lead to the repression of the ASS1 protein in the tumor, while in healthy tissue, the gene remains active and functional, therfore the increase of its production in healthy tissue. The multifunctional protein 1 interacts with the aminoacyl-tRNA synthetase (Q12904 AIMP1) and plays a role in gastric cancer, as well as stimulating the catalytic activity of the cytoplasmic arginyl-tRNA synthetase [39]. The protein 1, rich in cysteine and with a transmembrane domain (Q9H1C7 CYMST), when downregulated, can serve as a predictive biomarker for gastric intestinal metaplasia and CG [40].

In the CG-PCCs of signet ring cells of case 2, it is observed that the studied cysteines have higher quantification levels in healthy tissue, with the exception of the protein (Q9H1C7 CYSTM1). This protein, which is rich in cysteine and possesses protein 1 transmembrane domains, shows higher quantification values in tumor tissue. This could be indicative of tumor progression. However, in both intestinal like and not specified CG-PCC, the quantification value of CYSTM1 protein is higher in healthy tissue.

7.3. Sensitivity and Specificity of CBP (SDCBP and NCBP1) and (MGMT) Proteins

The highest sensitivity and specificity, precision and AUC, corresponds to SDCBP and MGMT proteins in intestinal CG-PCC and CG-PCC not specified, respectively. The presence of positive MGMT expression in gastric cancer has been recognized as an independent favorable prognostic factor. Including MGMT expression in the current TNM staging system could result in improved accuracy in prognostic predictions [41]. Helicobacter py. decreases the concentration of MGMT protein in gastric mucosal cells and induces methylation in CpG islands. When DNA damage is detect-

ed, methyl guanine methyl transferase transfers the methyl group from guanine to a cysteine of the same protein [42]. The four cases of GC-PGG were classified as stage III and IV. We have no information on whether cases 1, 2, and 3 had experienced any previous H. pylori gastric infection. But it is known that after H. pylori elimination, a significant reduction in the levels of MGMT methylation of CpG islands is observed in the gastric mucosa, while MGMT expression is increased [43]. In the DNA sequencing of the gastric tissue of Case 4, with CG-PCC of signet ring cells, mutation of the CREBBP gene has been observed, with variation of the amino acid Arginine by Cysteine. As a consequence of the mutation there has been a reassignment of arginine codons and enrichment of cysteine. The most common processes responsible for this type of point mutation, also known as missense mutation, can be induced by errors in RNA transcription, which generate messenger RNA with incorrect codons. One potential therapy for correcting pathogenic missense mutations involves the use of missense-correcting tRNAs (missense-correcting tRNAs)(mc-tRNAs). These t-mcRNAs are tRNAs specially designed, that are loaded with a specific amino acid but recognize different codons during translation. It has been shown that t-mcRNAs effectively correct missense mutations in the amino acids serine and arginine. The amino acid substitution has been confirmed by mass spectrometry, and the expression of the t-mcRNAs has been verified by sequencing [44]. A new option for the treatment of this patient would have been the use of mc-tRNAs to effectively correct missense mutations in the amino acids Arginine and Cysteine. A proteome-wide study has recently been carried out where peptides including disease-related amino acid mutations were analyzed, together with the intrinsically disordered regions of the human proteome. We identified 275 mutations associated with various diseases affecting 279 specific protein-protein interactions. Fifty percent of these mutations increase or create new binding motifs, while the other 50% decrease or disrupt them. In the analysis of the CREBBP gene, two main domains were highlighted: KIX and NCBD. The KIX domain is critical for interacting with transcription factors. It plays an important role in cell signaling. It is located in the central region of CREBBP and is associated with carcinogenic processes related to the PPI gene. It also facilitates interactions with several transcription factors. The NCBD interacts with disordered regions of other proteins, participating in several cell signaling pathways and modulating gene activation or silencing according to cellular signals [45]. The drug CCS1477 (Inobrodip), which is in a clinical trial for patients with advanced solid tumors, targets individuals with molecular markers indicating a potential favorable response to p300/CBP inhibition (NCT03568656 on ClinicalTrials.gov).

7.4. SDCBP, HIST1H4A and HDAC1 Proteins

Histones are nuclear proteins that maintain the nucleosome structure of chromatin in eukaryotic organisms. They play a central role in the regulation of transcription, DNA repair, DNA replication and chromosomal stability. The CREBBP gene encodes a protein that acts as a transcriptional coactivator through histone acetyltransferase type B (Q8WYB5) (HAT). This activity is critical in modulating chromatin structure and regulating gene transcription [46]. Histone acetyltransferase type B catalytic subunit (HAT) is performed by histone acetylation, which catalyzes the passage of an acetyl group to the lysine residue of the amino-terminal tail of the histone. This causes chromatin de-condensation, allowing gene transcription. In the proteomic analysis, this protein was not identified in GC-PCC cases 1, 2 and 3. HDACs remove acetyl groups from the -amino lysine residues of histone tails and effectively reduce transcription factor access by forming a closed chromatin conformation that alters the transcription of oncogenes and tumor suppressor genes [47]. The specific mutational profiles underlying in the particularly aggressive prognosis of intestinal GC-like and non-specific cells versus signet ring cells are due in part to mutations in the CREBBP gene [48]. Mutations or changes in the expression of HAT and HDAC are frequently observed in cancer cells. A loss-of-function mutation in the CBP/CREBBP gene, which encodes a HAT, is common in many types of cancer, including CG [49]. Mutations associated with the CREBBP gene may disrupt and reconfigure protein-protein interactions in case 4 with signet ring cell CG-PCC. GC-PCC cases 1, 2, 3, show higher histone acetyltransferase (HDAC) TU/SA ratio quantification values in tumor than in healthy tissue. Despite this, the HAT-1 enzyme was not detectable in the tissues of the CG-PCCs under study. The reduction in the activity of this enzyme could be due to variations in HAT-1 expression and activity levels, which vary according to tumor stage. It is likely that HAT1-mediated acetylation occurs early in the disease, during the early stages of tumor development. This may explain why in advanced GC (stages III and IV) of cases 1, 2 and 3, the enzyme responsible for histone de-acetylation has high levels of HDAC in the tumor tissue. Therapy with HDAC inhibitors of the Hippo/YAP pathway in cancer metastasis targets the transcriptional machinery [50]. The case 4 presented shows a somatic variant of the CREEBP gene in the CG-PCC of signet ring cells, which could result in changes in histone acetyltransferase (HDAC) expression. Dysregulation of HDAC includes cell differentiation, cell cycle alteration, angiogenesis, apoptosis, and autophagy. It has also been shown that histone acetylation at the promoters of p53-controlled genes, negatively regulates HDAC1. The expression of the p53 protein, a tumor suppressor protein, plays a crucial role in apoptosis or programmed cell death51. This is probably the reason why it was not possible to quantify the TP53 protein. SDCBP1 is an abundant protein in exosomes of different cellular origins, highlighting its potential use as a universal exosome biomarker [52]. In addition, P62805 Histone H4 (HIST1H4A) of the H4C1 gene is one of the most frequent proteins in extracellular vesicles. It is a protein-coding gene and a central component of nucleosomes. Negative regulation of Syndecan binding protein (SDCBP) plays a key role in tumorigenesis. SDCBP inhibits cell

proliferation and induces apoptosis by regulating the PI3K/AKT/mTOR signaling, in gastric carcinoma [53]. In the proteomic analysis of CG-PCC case 1, 2, 3, it was observed that the three proteins SDCBP, HDAC1 and HIST1H4A have their TU/SA ratio quantification values higher in tumor than in healthy tissue. The presence of HDAC deacetylase in signet ring cell GC-PCC cancer cells is a response to the previous increase in histone acetylation performed by HIST1H4A. This process seeks to counteract the mechanism that promotes acetylation-driven gene overexpression. The extracellular vesicle protein HIST1H4A could have been used as a biomarker for the early diagnosis of simple cancers [54].

7.5. Ubiquitin-Proteasome System (UPS)

This system modulates the stability of most intracellular proteins that are essential for functions such as metabolism, cell division and stress response, among other processes. In the ubiquitin-proteasome system (UPS), the enzymes E1 (ubiquitin activator), E2 (ubiquitin conjugator) and E3 (ubiquitin ligase) act in a coordinated manner to mark and transfer target proteins to the proteasome, where they will be degraded. This system is essential for maintaining protein balance within the cell, eliminating misfolded proteins and damaged organelles. In the study of GC development, it was observed dysfunction of the protein ubiquitination system (UPS), caused by abnormalities in E1, E2, and E3 enzymes. It resulted in the disproportionate accumulation of high protein levels [55]. The ubiquitin-conjugating enzyme E2 D3 (P61077) (UBE2D3) is involved in protein ubiquitination of small ribosomal subunits, P46783 (RPS10) and P60866 (RPS20), critical for quality control of ribosome-associated proteins [56]. BRG399, a small-molecule modulator of UBE2K, showed dose-dependent anticancer activity in an in vivo model of gastric cancer [57]. In intestinal like and not specified intestinal GC-PCC, the UBE2K protein has higher TU/SA ratio quantification values in tumor than in healthy tissue, while in signet ring cell GC-PCC it is higher in healthy tissue than in tumor. The cohort study conducted by retrospective whole exome sequencing in 186 paired tumor samples from Chinese patients with diffuse gastric cancer. It has been observed that, RNF213 gene has a variant incidence rate of 10% [58]. The E3 (Q63HN8) ubiquitin protein ligase (RNF213) has higher quantification values of the TU/SA ratio in healthy tissue than in tumor, in signet ring and not specified CG-PCCs. However, in the not specified ones the quantification of this protein is higher in the tumor. TP53, one of the mutated genes in case 4, can suppress antitumor immunity in GC59. The E3 ubiquitin/ISG15 (Q14258) protein ligase E3 (TRIM25) is involved in numerous cellular processes. TRIM25 overexpression may cause gastric cancer [60]. In intestinal like GC-PCC, the ratio of TU/SA quantification values of TRIM25 protein is higher in tumor than in healthy tissue. It has a sensitivity plus specificity of two, an accuracy of one and an AUC of one. This indicates that this protein could be a biomarker for diagnosis of ubiquitination system in GC-PCC.

7.6. Targeted Protein Degradation. PROTAC at CG-PCC

Recognition of a target protein by the ubiquitin-proteasome system (UPS) inside mammalian cells is achieved by protein degradation [61]. An alternative to targeted antitumor therapy is to mobilize its own protein degradation pathway by eliminating specific proteins from cells involved in tumor development. PROTACs are heterodifunctional molecules, consisting of a conjugate of the target protein of interest (usually an oncogenic or disease-related protein). It is a linker, which captures an E3 ubiquitin ligase, which marks the target protein for degradation. The cellular ubiquitin-proteasome system (UPS) performs the degradation function. Numerous PROTACs targeting gastrointestinal cancers have been successfully developed, and in many cases, their proteins of interest have been validated as clinical drug targets [62]. The potential role of PROTACs in GC-PCC targets oncogenic drivers such as CBP and TP53 proteins. For epigenetic dysregulation, they also used PROTACs. In CG-PCC, it is necessary to modify the molecular diagnostic and therapeutic strategy, since the results are so far not satisfactory. Technology has advanced, reducing the time required to perform sequencing tests and multi-omics analysis. The use of molecular diagnostics and targeted therapies such as PROTACs would be an essential complement to improve the medical and surgical management of this disease. Progress in multi-omics analysis have catalyzed a paradigm shift in cancer treatment, changing the focus from traditional organ-specific protocols to precision medicine [63]. From a surgical perspective, the difficulty of conducting clinical trials has been a disadvantage of oncologic surgery compared to medical oncology in recent years. Surgical therapy targeted by multi-omics analysis is also an innovative approach to cancer treatment, while diagnostics that identify specific molecular alterations play an essential role in targeting therapeutic options that could improve outcomes. The integration of different omics types captures the complexity of genetic variations that affect DNA and RNA and protein function. Similarly, epigenetic and metabolic analyses provide a more complete analysis of the cellular systems involved in the tumor microenvironment for tumor development and metastasis of gastric cancer. In addition, as observed in case 4, it is crucial to characterize the microbiome by immuno-histochemical techniques, which in this case allowed the identification of Helicobacter pylori. However, analysis of the microbiome by metagenomics would have identified the bacterium and host-microbiota interactions. The proteo-genomics analysis of early duodenal cancer reveals its cell pathways for carcinogenesis. These cell pathways differentiate from the pathways of low cohesive gastric cancer. Therefore, patients with lateral duodenal extension should be considered [23].

7.7. Limitations of the Study

The four cases analysed, despite the large amount of data provided by sequencing and proteomic analysis, are sparse. However, as a pilot study, it marks a way that could improve the surgical and

medical treatment of these patients in the near future. In the statistical analysis performed, another limitation of protein sensitivity and specificity, precision and AUC studies is not being able to eliminate false positives and negatives, which are common in proteomic datasets. In addition, it is sometimes difficult to understand the different sequencing data, as not all mutations or genetic variations cause changes in protein quantification levels. Another limitation is the lack of databases with large integrated multi-omics data sets and their interpretation. Multi-omics integration through artificial intelligence could facilitate the transition from epigenetic therapy to precision medicine [64]. Interdisciplinary collaboration could help support multi-omics teaching, research and clinical application globally. This could improve the diagnosis and treatment of these patients.

References

1. Nagtegaal ID, Odze RD, Klimstra D, Paradis V, Rugge M, Schirmacher P, et al. The 2019 WHO classification of tumours of the digestive system. Histopathology. 2020;76(2):182-188.
2. Li J. Gastric Cancer in Young Adults: A Different Clinical Entity from Carcinogenesis to Prognosis. Gastroenterol Res Pract. 2020; 2020: 9512707.
3. Drubay V, Nuytens F, Renaud F, Adenis A, Eveno C, Piessen G. Poorly cohesive cells gastric carcinoma including signet-ring cell cancer: Updated review of definition, classification and therapeutic management. World J Gastrointest Oncol. 2022;14(8):1406-1428.
4. Mariette C, Carneiro F, Grabsch HI, van der Post RS, Allum W, de Manzoni G, et al. Consensus on the pathological definition and classification of poorly cohesive gastric carcinoma. Gastric Cancer. 2019;22(1):1-9.
5. Guo YA, Chang MM, Huang W, Ooi WF, Xing M, Tan P, et al. Mutation hotspots at CTCF binding sites coupled to chromosomal instability in gastrointestinal cancers. Nat Commun. 2018;9(1):1520.
6. Barnes CE, English DM, Cowley SM. Acetylation & Co: an expanding repertoire of histone acylations regulates chromatin and transcription. Essays Biochem. 2019;63(1):97-107.
7. Gu M, Ren B, Fang Y, Ren J, Liu X, Wang X, et al. Epigenetic regulation in cancer. MedComm (2020). 2024;5(2): e495.
8. Zhu Y. Wang Z, Li Y, Peng H, Liu J, Zhang J, et al. The Role of CREBBP/EP300 and Its Therapeutic Implications in Hematological Malignancies. Cancers. 2023;15(4):1219.
9. Chen Q, Yang B, Liu X, Zhang XD, Zhang L, Liu T. Histone acetyltransferases CBP/p300 in tumorigenesis and CBP/p300 inhibitors as promising novel anticancer agents. Theranostics. 2022;12(11):4935-4948.
10. Koshiishi N, Chong JM, Fukasawa T, Ikeno R, Hayashi Y, Funata N, et al. p300 gene alterations in intestinal and diffuse types of gastric carcinoma. Gastric Cancer. 2004;7(2):85-90.
11. Zhao Z, Shilatifard A. Epigenetic modifications of histones in cancer. Genome Biol. 2019;20(1):245.
12. Yuan C, Zhang J, Deng C, Xia Y, Li B, Meng S, et al. Crosstalk of Histone and RNA Modifications Identified a Stromal-Activated Subtype with Poor Survival and Resistance to Immunotherapy in Gastric Cancer. Front Pharmacol. 2022; 13:868830.
13. Bednarz-Misa I, Fleszar MG, Fortuna P, Lewandowski Ł, Pasierb MM, Diakowska D, et al. Altered L-Arginine Metabolic Pathways in Gastric Cancer: Potential Therapeutic Targets and Biomarkers. Biomolecules. 2021;11(8):1086.
14. Shi LY, Wang YY, Jing Y, Xu MH, Zhu ZT, Wang QJ. Abnormal arginine metabolism is associated with prognosis in patients of gastric cancer. Transl Cancer Res. 2021;10(5):2451-2469.
15. Shitara K, Fleitas T, Kawakami H, Curigliano G, Narita Y, Wang F, et al. Pan-Asian adapted ESMO Clinical Practice Guidelines for the diagnosis, treatment and follow-up of patients with gastric cancer. ESMO Open. 2024;9(2):102226.
16. Gu M, Ren B, Fang Y, Ren J, Liu X, Wang X, et al. Epigenetic regulation in cancer. MedComm (2020). 2024;5(2): e495.
17. Tung KF, Pan CY, Chen CH, Lin WC. Top-ranked expressed gene transcripts of human protein-coding genes investigated with GTEx dataset. Sci Rep. 2020;10(1):16245.
18. Kasturirangan S, Nancarrow DJ, Shah A, Lagisetty KH, Lawrence TS, Beer DG, et al. Isoform alterations in the ubiquitination machinery impacting gastrointestinal malignancies. Cell Death Dis. 2024;15(3):194.
19. Cancer Genome Atlas Research Network. Comprehensive molecular characterization of gastric adenocarcinoma. Nature. 2014; 513(7517):202-9.
20. Yang J, Greally M, Strong VE, Coit DG, Chou JF, Capanu M, et al. Perioperative versus total neoadjuvant chemotherapy in gastric cancer. J Gastrointest Oncol. 2023;14(3):1193-1203.
21. Kim HD, Ryu MH, Kang YK. Adjuvant treatment for locally advanced gastric cancer: an Asian perspective. Gastric Cancer. 2024;27(3):439-450.
22. Fujitani K, Yang HK, Mizusawa J, Kim YW, Terashima M, Han SU, et al. Gastrectomy plus chemotherapy versus chemotherapy alone for advanced gastric cancer with a single non-curable factor (REGATTA): a phase 3, randomised controlled trial. Lancet Oncol. 2016;17(3):309-318.
23. Li L, Jiang D, Liu H, Guo C, Zhao R, Zhang Q, et al. Comprehensive proteogenomic characterization of early duodenal cancer reveals the carcinogenesis tracks of different subtypes. Nat Commun. 2023;14(1):1751.
24. Lee CM, Yoon SY, Park S, Park SH. Laparoscopic Whipple's Operation for Locally Advanced Gastric Cancer Invading the Pancreas and Duodenum: a Case Report. J Gastric Cancer. 2019;19(4):484-492.
25. Wang XB, Yang LT, Zhang ZW, Guo JM, Cheng XD. Pancreaticoduodenectomy for advanced gastric cancer with pancreaticoduodenal region involvement. World J Gastroenterol. 2008;14(21):3425-9.
26. Taube JM, Klein A, Brahmer JR, Xu H, Pan X, Kim JH, et al. Association of PD-1, PD-1 ligands, and other features of the tumor immune microenvironment with response to anti-PD-1 therapy. Clin

Cancer Res. 2014;20(19):5064-74.

27. Goodman AM, Kato S, Bazhenova L, Patel SP, Frampton GM, Miller V, et al. Tumor Mutational Burden as an Independent Predictor of Response to Immunotherapy in Diverse Cancers. Mol Cancer Ther. 2017;16(11):2598-2608.
28. Le DT, Uram JN, Wang H, Bartlett BR, Kemberling H, Eyring AD, et al. PD-1 Blockade in Tumors with Mismatch-Repair Deficiency. N Engl J Med. 2015;372(26):2509-20.
29. Yura M, Takano K, Adachi K, Hara A, Hayashi K, Tajima Y, et al. Pancreaticoduodenectomy after neoadjuvant chemotherapy for gastric cancer invading the pancreatic head: A case report. World J Gastroenterol. 2021;27(6):534-544.
30. Janjigian YY, Kawazoe A, Bai Y, Xu J, Lonardi S, Metges JP, et al. Investigators. Pembrolizumab plus trastuzumab and chemotherapy for HER2-positive gastric or gastro-oesophageal junction adenocarcinoma: interim analyses from the phase 3 KEYNOTE-811 randomised placebo-controlled trial. Lancet. 2023;402(10418):2197-2208.
31. He Y, Wang X. Identification of molecular features correlating with tumor immunity in gastric cancer by multi-omics data analysis. Ann Transl Med. 2020;8(17):1050.
32. Binnewies M, Roberts EW, Kersten K, Chan V, Fearon DF, Merad M, et al. Understanding the tumor immune microenvironment (TIME) for effective therapy. Nat Med. 2018;24(5):541-550.
33. Qian B, Yao Z, Yang Y, Li N, Wang Q. Downregulation of SDCBP inhibits cell proliferation and induces apoptosis by regulating PI3K/AKT/mTOR pathway in gastric carcinoma. Biotechnol Appl Biochem. 2022;69(1):240-247.
34. Liu L, Lang Z, Wang P, Wang H, Cao Y, Meng X, et al. The nucleosome binding protein 1 promotes the growth of gastric cancer cells. J Cancer. 2019;10(5):1132-1137.
35. Wang F, Chen S, Peng S, Zhou X, Tang H, Liang H, et al. PRMT1 promotes the proliferation and metastasis of gastric cancer cells by recruiting MLXIP for the transcriptional activation of the β-catenin pathway. Genes Dis. 2023;10(6):2622-2638.
36. Álvarez MC, Santos JC, Maniezzo N, Ladeira MS, da Silva AL, Scaletsky IC, et al. MGMT and MLH1 methylation in Helicobacter pylori-infected children and adults. World J Gastroenterol. 2013;19(20):3043-51.
37. Zappe K, Pühringer K, Pflug S, Berger D, Böhm A, Kreinecker SS, et al. Association between MGMT Enhancer Methylation and MGMT Promoter Methylation, MGMT Protein Expression, and Overall Survival in Glioblastoma. Cells. 2023;12(12):1639.
38. Tsai CY, Chi HC, Chi LM, Yang HY, Tsai MM, Lee KF, et al. Argininosuccinate synthetase 1 contributes to gastric cancer invasion and progression by modulating autophagy. FASEB J. 2018;32(5):2601-2614.
39. Zhou Z, Sun B, Huang S, Yu D, Zhang X. Roles of aminoacyl-tRNA synthetase-interacting multi-functional proteins in physiology and cancer. Cell Death Dis. 2020;11(7):579.
40. Eskandarion MR, Eskandarieh S, Farahani AS, Mahmoodzadeh H, Shahi F, Oghabian MA, et al. Prediction of novel biomarkers for gastric intestinal metaplasia and gastric adenocarcinoma using bioinformatics analysis. Heliyon. 2024;10(9): e30253.
41. Cao Y, Liu H, Li H, Lin C, Li R, Wu S, et al. Association of O6-Methylguanine-DNA Methyltransferase Protein Expression with Postoperative Prognosis and Adjuvant Chemotherapeutic Benefits Among Patients with Stage II or III Gastric Cancer. JAMA Surg. 2017;152(11): e173120.
42. Sepulveda AR, Yao Y, Yan W, Park DI, Kim JJ, Gooding W, et al. CpG methylation and reduced expression of O6-methylguanine DNA methyltransferase is associated with Helicobacter pylori infection. Gastroenterology. 2010;138(5):1836-44.
43. Muhammad JS, Eladl MA, Khoder G. Helicobacter pylori-induced DNA Methylation as an Epigenetic Modulator of Gastric Cancer: Recent Outcomes and Future Direction. Pathogens. 2019;8(1):23.
44. Hou Y, Zhang W, McGilvray PT, Sobczyk M, Wang T, Weng SHS, et al. Engineered mischarged transfer RNAs for correcting pathogenic missense mutations. Mol Ther. 2024;32(2):352-371.
45. Kliche J, Simonetti L, Krystkowiak I, Kuss H, Diallo M, Rask E, et al. Proteome-scale characterisation of motif-based interactome rewiring by disease mutations. Mol Syst Biol. 2024;20(9):1025-1048.
46. Yu X, Zhao H, Wang R, Chen Y, Ouyang X, Li W, et al. Cancer epigenetics: from laboratory studies and clinical trials to precision medicine. Cell Death Discov. 2024;10(1):28.
47. Li Y, Seto E. HDACs and HDAC Inhibitors in Cancer Development and Therapy. Cold Spring Harb Perspect Med. 2016;6(10): a026831.
48. Pelaez JG, Matos RB, Gullo I, Carneiro F, Oliveira C. Histological and mutational profile of diffuse gastric cancer: current knowledge and future challenges. Mol Oncol. 2021;15(11):2841-2867.
49. Ogiwara H, Sasaki M, Mitachi T, Oike T, Higuchi S, Tominaga Y, et al. Targeting p300 Addiction in CBP-Deficient Cancers Causes Synthetic Lethality by Apoptotic Cell Death due to Abrogation of MYC Expression. Cancer Discov. 2016;6(4):430-45.
50. Zhou T, Li X, Liu J, Hao J. The Hippo/YAP signaling pathway: the driver of cancer metastasis. Cancer Biol Med. 2023;20(7):483-9.
51. Peluso AA, Kempf SJ, Verano-Braga T, Rodrigues-Ribeiro L, Johansen LE, Hansen MR, et al. Quantitative Phosphoproteomics of the Angiotensin AT2-Receptor Signaling Network Identifies HDAC1 (Histone-Deacetylase-1) and p53 as Mediators of Antiproliferation and Apoptosis. Hypertension. 2022;79(11):2530-2541.
52. Kugeratski FG, Hodge K, Lilla S, McAndrews KM, Zhou X, Hwang RF, et al. Quantitative proteomics identifies the core proteome of exosomes with syntenin-1 as the highest abundant protein and a putative universal biomarker. Nat Cell Biol. 2021;23(6):631-641.
53. Qian B, Yao Z, Yang Y, Li N, Wang Q. Downregulation of SDCBP inhibits cell proliferation and induces apoptosis by regulating PI3K/AKT/mTOR pathway in gastric carcinoma. Biotechnol Appl Biochem. 2022;69(1):240-247.
54. Ferguson S, Yang KS, Weissleder R. Single extracellular vesicle analysis for early cancer detection. Trends Mol Med. 2022;28(8):681-692.

55. Yang H, Ai H, Zhang J, Ma J, Liu K, Li Z. UPS: Opportunities and challenges for gastric cancer treatment. Front Oncol. 2023; 13:1140452.

56. Yalçin Z, Koot D, Bezstarosti K, Salas-Lloret D, Bleijerveld OB, Boersma V, et al. Ubiquitinome Profiling Reveals in Vivo UBE2D3 Targets and Implicates UBE2D3 in Protein Quality Control. Mol Cell Proteomics. 2023;22(6):100548.

57. Kazerounian S: BRG399, a small molecule modulator of UBE2K demonstrated dose-dependent anti-cancer efficacy in an in vivo model for gastric cancer. Cancer Res (2022) 82 (12_Supplement): 5320.

58. Liu ZX, Zhang XL, Zhao Q, Chen Y, Sheng H, He CY, et al. Whole-Exome Sequencing Among Chinese Patients With Hereditary Diffuse Gastric Cancer. JAMA Netw Open. 2022;5(12): e2245836.

59. He Y, Wang X. Identification of molecular features correlating with tumor immunity in gastric cancer by multi-omics data analysis. Ann Transl Med. 2020;8(17):1050.

60. Tesiye MR, Zaersabet M, Salehiyeh S, Jafari SZ. The role of TRIM25 in the occurrence and development of cancers and inflammatory diseases. Biochim Biophys Acta Rev Cancer. 2023;1878(5):188954.

61. Taylor JD, Barrett N, Cuesta SM, Cassidy K, Pachl F, Dodgson J, et al. Targeted protein degradation using chimeric human E2 ubiquitin-conjugating enzymes. Commun Biol. 2024;7(1):1179.

62. Chen Y, Yang Q, Xu J, Tang L, Zhang Y, Du F, et al. PROTACs in gastrointestinal cancers. Mol Ther Oncolytics. 2022; 27:204-223.

63. Mechahougui H, Gutmans J, Colarusso G, Gouasmi R, Friedlaender A. Advances in Personalized Oncology. Cancers (Basel). 2024;16(16):2862.

64. He X, Liu X, Zuo F, Shi H, Jing J. Artificial intelligence-based multi-omics analysis fuels cancer precision medicine. Semin Cancer Biol. 2023; 88:187-200.